The effect of angular velocity-dependent Sagnac effect on speckle pattern images

HUSAMETTIN SERBETCI[1,*], EGE INCE[2], ISA NAVRUZ[3]
[1]Department of Electrical and Electronics Engineering, Cankiri Karatekin University, 18100 Cankiri, Turkey
[2]Graduate School of Natural and Applied Sciences, Ankara University, 06110 Ankara, Turkey
[3]Department of Electrical and Electronics Engineering, Ankara University, 06100 Ankara, Turkey

In this study, a novel optical gyroscope design is proposed as an alternative to the conventional fiber optic gyroscope configuration. In the proposed design, a multimode optical fiber is used instead of a single-mode optical fiber. Multimode optical fibers produce a speckle pattern image at their output. It has been experimentally demonstrated that this design, which utilizes speckle pattern imaging captured by a CCD camera, can be employed to measure angular velocity. The detection of velocity is achieved through correlation analysis of the speckle pattern images observed at the output of the multimode fiber. Prior to the experimental study, the sensitivity of the speckle pattern emerging in the fiber cross-section to changes in angular velocity was simulated using the beam propagation method. Subsequently, all components of the proposed optical gyroscope system were assembled on a vibration-free optical table and tested at different angular velocities. Both simulation and experimental studies reveal that the speckle pattern images generated at the output of the multimode optical fiber can be utilized to measure changes in angular velocity.

1. Introduction

Precise angular velocity measurements are of great importance in various application areas such as navigation, guidance, and stabilization. Traditional mechanical gyroscopes, due to the presence of moving parts, face issues over time such as wear, friction-induced errors, and thermal expansion. To overcome these problems, fiber optic gyroscopes (FOGs) have been developed and widely adopted due to their high precision, low maintenance requirements, and long operational life. FOGs are optical devices that perform angular velocity measurements based on the Sagnac effect.

The Sagnac effect is based on the formation of a phase shift in light traveling within a rotating reference frame, depending on the direction of motion. In FOGs, this effect is obtained by propagating light in opposite directions along a closed optical path. The phase difference between the two counter-propagating light beams is directly related to the rotation rate of the system, and this phase difference is measured using optical interferometry techniques to determine angular velocity. Although traditional FOG systems achieve high precision by using single-mode fibers, the system's performance is affected by factors such as fiber length, the stability of optical components, and susceptibility to external influences.

In recent years, various studies have been conducted on alternative sensing methods to enhance the performance of FOGs. Nearly all FOGs presented in the literature rely on the principle of measuring the phase difference induced by the Sagnac effect in single-mode fibers. In this study, a

significantly different technique from that used in conventional FOGs is proposed. It is demonstrated that a new FOG system can be developed by imaging the speckle pattern at the output of multimode fibers. At the output end of this fiber illuminated by a laser, an interference pattern of light, referred to as a speckle pattern, emerges due to interference between modes. Based on the assumption that this speckle pattern could be sensitive to angular velocity variations, similar to the Sagnac effect, a system was designed, and both simulation and experimental studies were conducted. Instead of using a single-mode fiber and photodetector, the speckle patterns imaged using a multimode step-index fiber and a camera were analyzed. The results show that the simulations and experimental studies are consistent. This research proves that speckle pattern imaging-based FOGs can provide an alternative to conventional interferometric methods for measuring angular velocity.

2. Theory

The fundamental operating principle of FOGs is based on the Sagnac effect. The Sagnac effect refers to the phenomenon in which light propagating through a rotating loop experiences a phase shift along a circular optical path. In a fiber optic gyroscope, a light beam from a coherent light source is split into two by a beam splitter and propagates in opposite directions along a fiber loop. When the plane of the gyroscope is rotated, a phase difference arises between the two light beams. This phase difference

results in an interferometric pattern and is directly related to the angular velocity of the rotating gyroscope plane. At the output of the gyroscope, this phase difference leads to a change in the light intensity detected by the photodetector. By analyzing the detector signal, the angular velocity can be measured [1-3].

The sensitivity of FOGs depends on the fiber length, the wavelength, and noise factors within the system. To improve the sensitivity and accuracy of the system, ongoing research focuses on enhancing the performance of FOGs using polarization-maintaining fibers [4], low-loss optical components [5] and various optimization techniques [6, 7].

The speckle pattern imaging technique proposed in this study is an interferometric measurement method that has been demonstrated in the literature for the detection of physical quantities such as refractive index [8-11], temperature [12,13], magnetic field [14,15], displacement [16-18], strain [19-21], and force [22, 23] as well as in spectrometer applications [24-26]. In this technique, which employs multimode step-index fibers, an interference pattern known as a speckle pattern is formed at the fiber output as a result of the interference between hundreds of guided modes within the fiber. The speckle pattern image, which represents the light intensity distribution over the fiber cross-section in the X-Y plane, denoted as $I(x, y)$, can be calculated by summing the complex field amplitudes of each fiber mode, as given in equation 1.

$$I_0(x, y) = \sum_{m=0}^{M} \sum_{n=0}^{M} a_{0m} a_{0n} \exp\{j[\emptyset_{0m} - \emptyset_{0n}]\} \quad (1)$$

Here, $a_{0m}(x, y)$ and $\emptyset_{0m}(x, y)$ represent the amplitude and phase distributions, respectively, of the m-th mode over the fiber cross-sectional surface. Environmental factors such as temperature, strain, vibration, and displacement alter the phase and amplitude of the modes guided within the fiber and consequently affect the speckle pattern image. Under the influence of such a factor, the resulting light intensity distribution over the X-Y plane can be calculated using equation 2.

$$I(x, y) = \sum_{m=0}^{M} \sum_{n=0}^{M} \begin{matrix} (a_{0m} + \Delta a_m)(a_{0n} + \\ \Delta a_n) \end{matrix} \exp\{j[\emptyset_{0mn} + \Delta\emptyset_{mn}]\} \quad (2)$$

Here, Δa_m and $\Delta\emptyset_m$ represent the amplitude and phase changes, respectively, caused by environmental effects. The speckle pattern image is the result of the amplitude and phase distributions of the modes guided within the fiber. Variations in this image are highly sensitive to the amplitude and phase of each mode. It is a well-established fact that, due to the Sagnac effect, a phase difference occurs between the fundamental modes of two counter-propagating light beams in an optical fiber loop. Similarly, it can be predicted that a change in the speckle patterns will occur due to the Sagnac effect in a loop utilizing a

multimode fiber. In optical fiber sensors that use speckle pattern images for sensing, methods such as correlation analysis [8, 9, 11], NIPC [16, 27, 28], and deep learning [29, 30] have been employed in the literature. In this study, the change in speckle patterns recorded while the fiber loop is rotating, and its relationship with angular velocity, is determined using the correlation coefficient (CC) given in equation 3.

$$CC = \frac{\sum(M_i - \bar{M})(N_i - \bar{N})}{\sqrt{\sum(M_i - \bar{M})^2 \sum(N_i - \bar{N})^2}} \quad (3)$$

In the equation, M and N represent the reference and the compared image, respectively, while $\bar{M}$ and $\bar{N}$ denote their respective mean values. In the first step of the sensing process, the reference image is determined. The reference image is the speckle pattern recorded when the system is stationary ($\Omega = 0$ rad/s). Subsequently, the CC is calculated between the reference image and the speckle pattern image obtained after applying angular velocity to the system. The sensing process is carried out by analyzing the variations in the CC values.

A more precise sensing can be achieved if the variations in the speckle pattern images can be more effectively correlated with the angular velocity. To accomplish this, a series of image preprocessing steps were applied to the speckle pattern images. First, due to the cylindrical structure of the fiber, the speckle pattern appears in a circular region; therefore, cropping and masking operations were applied to remove the area outside the circle. Next, background illumination correction was performed to enhance speckle visibility and eliminate non-uniform light distribution. As a result of these processes, a more accurate correlation between speckle pattern changes and angular velocity was achieved, leading to improved sensing performance.

In the speckle pattern-based fiber optic gyroscope system proposed in this study, unlike conventional methods, an optical phase modulator is not required. An illustration of the proposed gyroscope system is presented in Fig. 1. The system consists of a laser light source emitting at a wavelength of 635 nm (Thorlabs LDM635), an 80-meter-long step-index multimode fiber (Thorlabs FG105LCA), a CCD camera (Thorlabs BC106-VIS), and a 2x2 50:50 multimode optical coupler.

In the system illustrated in the figure, all components except the computer are mounted on a rotating platform. The light emitted from the laser passes through the optical coupler and is split into two arms propagating in opposite directions around the fiber loop. When the platform is stationary, the image captured by the camera is labeled as the reference speckle pattern image. As the platform rotates, the speckle pattern image begins to change in relation to the angular velocity. This variation in the image is converted into numerical data through correlation analysis, and the sensing process is thereby carried out.
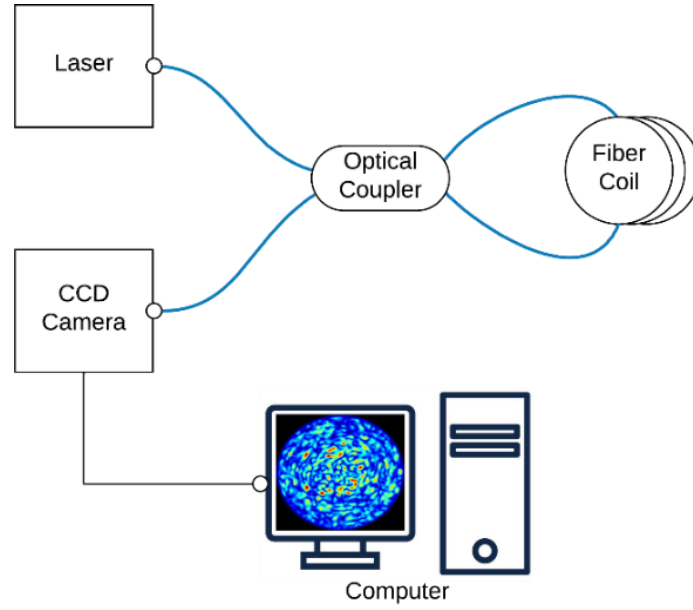
Fig. 1. Illustration of the proposed gyroscope system (colour online)

3. Simulation studies

To investigate the variation of the recorded speckle pattern images with angular velocity in the proposed gyroscope system, simulation studies were carried out using the Beam Propagation Method (BPM). A step-index multimode fiber with a length of 20120 μm and core and cladding refractive indices of 1.45 and 1.4332, respectively, was designed. The designed fiber has a core/cladding diameter of 105/125 μm, and the laser wavelength used in the simulations was 635 nm. Based on these parameters and using Bessel functions, the number of supported modes was calculated, and it was found that the fiber can guide approximately 1580 LP modes. The speckle pattern image formed at the output of the fiber with length 20120 μm is presented in Fig. 2.
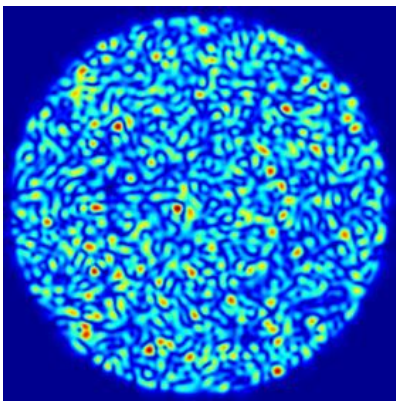
Fig. 2. Numerically calculated speckle pattern image (colour online)

During the simulation process, speckle pattern images in the x-y plane were recorded along with amplitude and phase information at every 0.5 μm step along the z-axis, which is the direction of light propagation. The Sagnac effect causes an optical path difference between two light beams propagating in opposite directions within an optical fiber. To simulate a phase difference similar to the Sagnac effect between two co-propagating beams along a straight fiber, the point at 20060 μm along the z-axis, where the optical path difference is zero ($\Delta L = 0$), was selected as the reference point. Subsequently, speckle pattern images were calculated and recorded at every 0.5 μm step forward and backward from this reference point. A total of 241 images, including the reference, were obtained in the range of 20000–20120 μm. Fig. 3 shows the optical path lengths symmetrically positioned relative to the reference point and the locations at which the speckle pattern images were computed.

As an example, calculation, at the positions 20057 μm and 20063 μm along the z-axis of the selected fiber, the optical path length of the light is 3 μm longer than the reference point for one beam and 3 μm shorter for the other, both originating from the same source. Thus, the total optical path difference between the two beams ($2\Delta L$) becomes 6 μm. The speckle pattern images recorded with amplitude and phase information can be summated by taking the reference point as the axis of symmetry. The resulting new speckle pattern images are labeled as the speckle patterns corresponding to the optical path differences. Fig. 4 shows the dataset consisting of the speckle pattern images and their associated optical path differences.
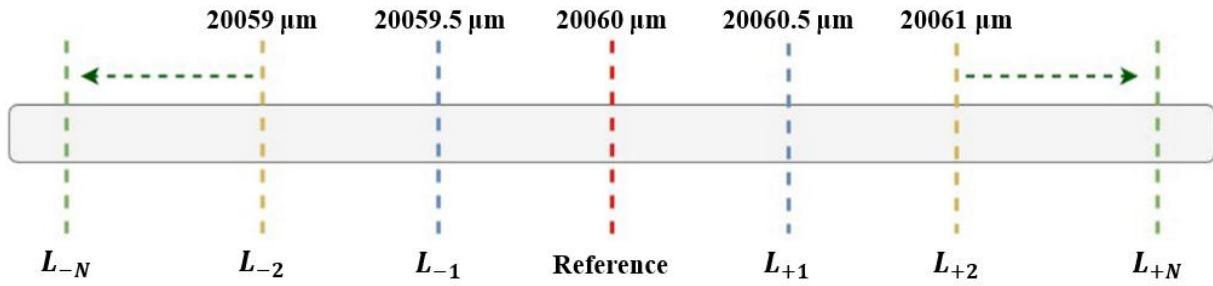
Fig. 3. Symmetrical distribution of optical path differences with respect to the reference point and the corresponding positions where speckle pattern images were computed along the fiber axis (colour online)
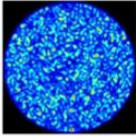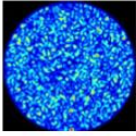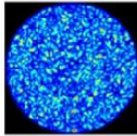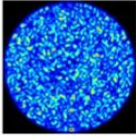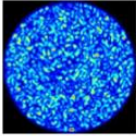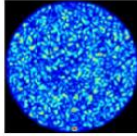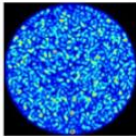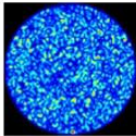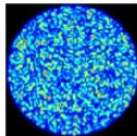

Fig. 4. Dataset composed of speckle pattern images and their corresponding optical path differences calculated along the multimode fiber (colour online)

As in conventional fiber optic gyroscopes, a phase difference arises between two counter-propagating light beams on a rotating platform due to the Sagnac effect. In the system designed to observe a similar effect along a straight fiber, the phase differences are represented by different optical path lengths determined relative to a reference point. In this system, the variations in the speckle pattern images computed at different path lengths were quantified using correlation analysis. Fig. 5 presents the graph of optical path difference-correlation coefficient.

In Fig. 5, it is observed that changes in the CC become measurable for optical path differences of 35 μm and above. For optical path differences smaller than approximately 35 μm, the modal phase shifts are insufficient to cause significant intensity redistribution in the speckle pattern, and thus the CC remains nearly constant. When the optical

path difference exceeds this threshold, the phase variation becomes large enough to alter the speckle structure, resulting in a measurable decrease in CC.

The simulation study demonstrates that the speckle pattern formed by two light beams propagating in the same direction along a straight fiber varies with the optical path difference. In a setup configured as a fiber loop, two counter-propagating light beams can generate speckle pattern images at the output that change according to the optical path difference. Such a system can be used to measure angular velocity. Moreover, by increasing the number of turns of the fiber coil, the optical path difference-correlation change can be accelerated and thus a fiber optic gyroscope system with higher sensitivity to angular velocity can be designed.
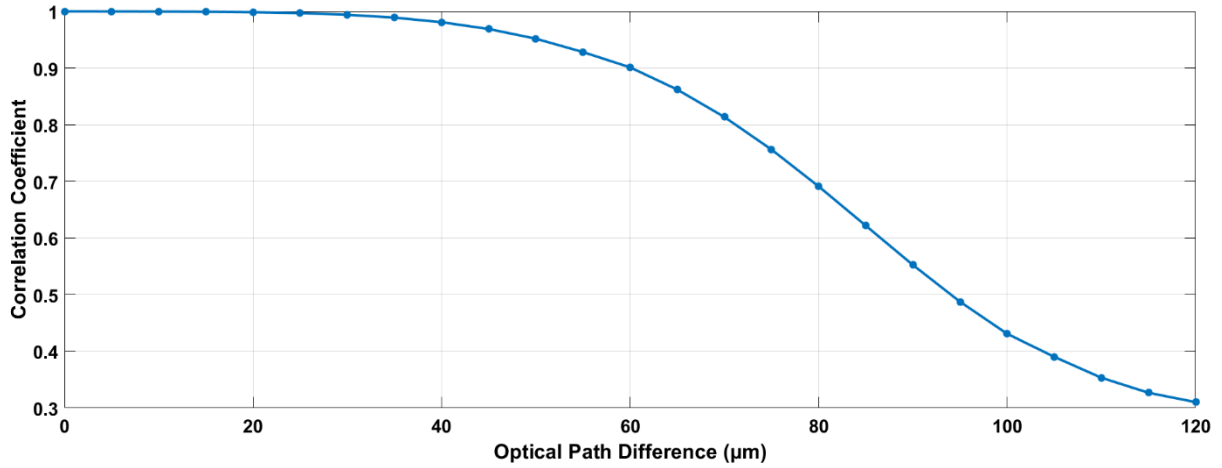
Fig. 5. Illustrating the relationship between optical path difference and correlation coefficient (colour online)

4. Experimental studies

To experimentally realize the speckle pattern-based FOG structure, a rotational table system was installed on a vibration-free optical table. The fiber coil, laser light source, CCD camera, and optical coupler were fixed onto the table to form the FOG system illustrated in Fig. 1.

The optical modes generated by the laser source were split into two optical paths in a 50:50 ratio using a multimode coupler and directed to both ends of the fiber coil. The two light beams propagating in opposite directions within the coil interfere upon returning to the optical coupler, and this interference is observed as a speckle pattern image by the CCD camera. When the rotational table is stationary, no phase difference occurs between the counter-propagating light beams, and the speckle pattern image recorded under these conditions is labeled as the reference image.

After recording the reference speckle pattern image, successive images were captured for 10 minutes under the stationary condition of the rotational table to test stability. At the end of this period, the correlation coefficient between the reference image and the recorded speckle pattern images dropped to approximately 0.93. This value means that the deviation in CC is 0.07 when the system is stationary for 10 minutes. Since the angular velocity measurement does not exceed 30 seconds after a reference image is recorded in the experimental studies, this deviation is negligible.

Experimental studies were started by recording the reference image. In experiments conducted by applying three different speed tests in which the rotational table reached angular velocities of 3.31 rad/s, 2.99 rad/s, and 2.51 rad/s, speckle pattern images were recorded every two seconds. While capturing the images, the instantaneous angular velocity of the rotational table was simultaneously measured. The speckle pattern images recorded for different angular velocity trials were analyzed. In Fig. 6, the angular velocity-time variation (red) and the correlation coefficient-time variation (blue) are shown.

As shown in Fig. 6.a, the angular velocity of the rotational table, which remained stationary for the first few seconds, reached a maximum of 2.51 rad/s at the 12th second and was then decelerated in a controlled manner, becoming to a stationary at the 24th second. At the moment when the angular velocity was highest, the CC dropped to 0.6878. When the turntable stopped moving, this value increased to 0.92.

In Fig. 6 (b) and (c), it is observed that the same gyroscope system exhibits a similar characteristic variation of CC for different angular velocities. As the angular velocity increases, the Sagnac effect produces larger phase differences between the counter-propagating beams, which leads to more pronounced changes in the speckle structure. Consequently, the correlation coefficient decreases further at higher angular velocities due to the stronger decorrelation of the recorded speckle patterns. In these two graphs, the rotational table was accelerated to maximum angular velocities of 2.99 rad/s and 3.31 rad/s, respectively, and the CC at these moments were calculated as 0.5984 and 0.531. The experimental studies conducted for three different angular velocities have demonstrated that as the angular velocity increases, the similarity of the speckle pattern images to the reference image decreases, and therefore, the CC decreases.

The correlation coefficient-angular velocity graphs clearly show an inverse relationship between the CC and angular velocity. The fact that the instantaneous angular velocity is associated with changes in the CC demonstrates that this system can function as an optical gyroscope, as validated by both simulation and experimental results.

The proposed multimode fiber-based FOG offers several advantages over traditional systems, including the elimination of an optical phase modulator and high-precision photodetectors, which simplifies the architecture and reduces cost. Moreover, the camera-based speckle pattern analysis provides richer spatial information that can be exploited with advanced processing techniques, offering enhanced sensitivity and the potential for multi-parameter sensing.

In this study, a limited number of experimental tests were conducted based on the length of the fiber used in the gyroscope system and the maximum angular velocity

achievable by the rotational table. Experimental studies can be improved by using a larger number of fiber coil loops and a rotary table that can reach higher angular velocities. The effect of the number of coil loops on angular velocity sensitivity and the maximum and minimum angular velocity limits measurable by the system can be investigated. Additionally, factors that may enhance system performance, such as increasing camera resolution or using different optical fibers that provide more pronounced speckle patterns, can also be explored. These suggestions will be addressed in future studies.
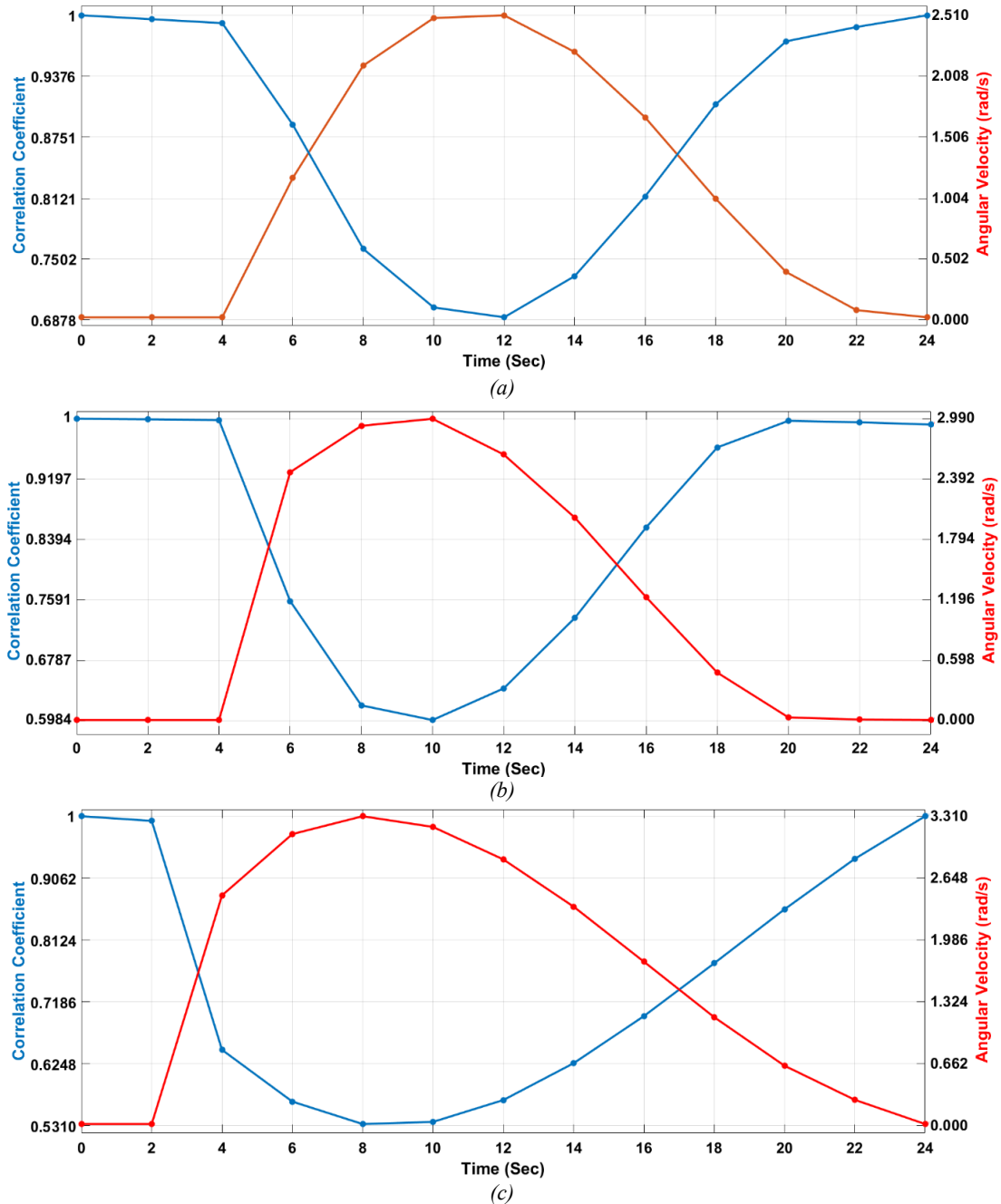

Fig. 6. Angular velocity and correlation coefficient variations over time during experiments with rotational table speeds of (a) 2.51 rad/s, (b) 2.99 rad/s and (c) 3.31 rad/s (colour online)

5. Conclusions

In this study, a novel optical gyroscope system that utilizes a multimode fiber and a camera has been proposed as an alternative to the conventional FOG architecture. The system's capability to measure angular velocity was investigated through both simulations and experimental studies. In the proposed system, the variations in speckle pattern images recorded at the output of the multimode fiber were evaluated as a function of angular velocity, and the similarity between images was quantitatively analyzed using the CC.

The results obtained from the system tested at different angular velocities demonstrated that the CC, which reflects the changes in the speckle patterns, varies inversely with angular velocity. The variation of speckle patterns indicates that the proposed system can be used as a FOG for measuring angular velocity. The results reveal that this system, based on speckle pattern imaging and designed with a multimode fiber, is a strong candidate for the class of FOGs. The performance of the proposed system can be further improved by using a high-resolution camera, increasing the number of loop, or using different optical fibers that generate more speckle patterns.

References

[1] X. Zhang, H. Ma, K. Zhou, Z. Jin, Optical Fiber Technology **13**(2), 135 (2007).

[2] H. Ma, Y. Chen, M. Li, Z. Jin, Applied Optics **49**, 6253 (2010).

[3] R. M. Khoshki, S. Ganesan, International Journal of Hybrid Information Technology **7**(5), 23 (2014).

[4] H. Li, X. Li, D. Xu, J. Wang, H. Yang, Journal of Lightwave Technology **41**(8), 2547 (2023).

[5] S. Gundavarapu, M. Belt, T. A. Huffman, M. A. Tran, T. Komljenovic, J. E. Bowers, D. J. Blumenthal, Journal of Lightwave Technology **36**(4), 1185 (2018).

[6] W. Wang, X. Chen, Applied Optics **55**(23), 6243 (2016).

[7] L. Wang, H. Li, J. Zhang, H. Ma, Z. Jin, Optics Communications **387**, 18 (2017).

[8] H. Şerbetçi, I. Navruz, F. Ari, Ain Shams Engineering Journal **15**, 103122 (2024).

[9] F. Ari, H. Şerbetçi, İ. Navruz, Optical Fiber Technology **79**, 103366 (2023).

[10] A. Theodosiou, IEEE Sensors Journal **24**(1), 287 (2024).

[11] H. Serbetci, I. Navruz, F. Ari, 30th Signal Processing and Communications Applications Conference (SIU), 2022.

[12] J. Wang, S. Yan, F. Xu, 16th International Conference on Optical Communications and Networks (ICOCN), 2017.

[13] V. Trivedi, S. Mahajan, V. Chhaniwal, Z. Zalevsky, B. Javidi, A. Anand, Sensors and Actuators A: Physical **216**, 312 (2014).

[14] R. Z. Zhu, S. J. Wan, Y. F. Xiong, H. G. Feng, Y. Chen, Y. Lu, F. Xu, Journal of Lightwave Technology **39**(11), 3614 (2021).

[15] T. D. Cabral, D. F. Franco, E. Fujiwara, M. Nalin, C. M. B. Cordeiro, IEEE Sensors Journal **23**(7), 6872 (2023).

[16] Y. Liu, Q. Qin, H. Liu, Z. Tan, M. Wang, Optical Fiber Technology **46**, 48 (2018).

[17] W. Chen, F. Feng, D. Chen, W. Lin, S. C. Chen, Sensors and Actuators A: Physical **296**, 1 (2019).

[18] J. H. Osório, T. D. Cabral, E. Fujiwara, M. A. R. Franco, F. Amrani, F. Delahaye, C. M. B. Cordeiro, Optical Fiber Technology **78**, 103335 (2023).

[19] M. J. Murray, A. Davis, C. Kirkendall, B. Redding, Optics Express **27**(20), 28494 (2019).

[20] M. J. Murray, B. Redding, Optics Letters **45**(6), 1309 (2020).

[21] H. Şerbetçi, I. Navruz, F. Ari, Optoelectron. Adv. Mat. **19**(1-2), 17 (2025).

[22] E. Fujiwara, Y. T. Wu, M. F. M. dos Santos, E. A. Schenkel, C. K. Suzuki, Sensors and Actuators A: Physical **263**, 677 (2017).

[23] A. Garcia-Valenzuela, M. Tabib-Azar, Sensors and Actuators A: Physical **36**, 199 (1993).

[24] B. Redding, S. M. Popoff, H. Cao, Optics Express **21**(5), 6584 (2013).

[25] B. Redding, S. M. Popoff, Y. Bromberg, M. A. Choma, H. Cao, Applied Optics **53**(3), 410 (2014).

[26] F. Feng, J. Gan, P. F. Chen, W. Lin, G. Y. Chen, C. Min, M. Somekh, Optics Communications **522**, 128675 (2022).

[27] E. Fujiwara, M. F. Marques dos Santos, C. K. Suzuki, Applied Optics **56**(6), 1585 (2017).

[28] E. Fujiwara, Y. T. Wu, C. K. Suzuki, Optics and Lasers in Engineering **50**(12), 1726 (2012).

[29] U. Kürüm, P. R. Wiecha, R. French, O. L. Muskens, Optics Express **27**(15), 20965 (2019).

[30] Y. Li, Y. Xue, L. Tian, Optica **5**(10), 1181 (2018).

_____

*Corresponding author: hserbetci@karatekin.edu.tr